Chapter 13

The Electrostatic Quadrupoles (ESQ) and Beam Collimators

13.1 Introduction

The Electrostatic Focusing Quadrupoles (ESQ) in the $(g-2)$ storage ring are used to confine muons vertically. The ESQ were first used for beam storage in the final muon $(g-2)$ experiment at CERN [1], and in the muon $(g-2)$ experiment E821 at BNL [2]. Our baseline plan for E989 is to reuse the existing E821 ESQ after careful refurbishment and necessary upgrades as will be discussed in the following sections. This decision was made after we have carefully considered alternatives, e.g., weak magnetic focusing, and alternating skew electrostatic quad focusing.

13.2 Requirements for ESQ and Beam Collimators

The E989 ESQ must

1. Produce vertically focusing electrostatic quadrupole field in the muon storage region.

2. Have operating point in resonance-free region around $n = 0.185$.

3. Have stable operation during extended periods of time in a vacuum of 10^{-6} Torr or better.

4. Have reliable operation in pulsed mode with time structure of the beam as described in section 7.2 (12 Hz average rate of muon spills that comprises sequences of four consecutive spills with 10 ms spill-separations).

5. Be optimized for muon storage efficiency.

6. Have minimum possible amount of material at places where the trajectories of incoming muons and decay positrons intercept the parts of ESQ.

7. The quality as well as long- and short-term stability of the electrostatic quadrupole field must be sufficient to keep the beam-dynamics systematic uncertainties well below the E989 goal.

The E989 ESQ and Beam Collimators must

1. Provide effective scraping of the injected beam to remove muons outside the storage region.

2. Be made from non-magnetic materials to not deteriorate the quality of the dipole storage magnetic field.

3. The thickness and the shape of collimators must be optimized to satisfy the two conflicting requirements *i)* efficiently remove muons outside the storage region and *ii)* has little effect (e.g. multiple scattering, showering, etc.) to the decay positrons.

13.3 Design of ESQ

Since we are planning to reuse the E821 quadrupoles for E989, the basic features of the mechanical and electrical design of ESQ in E989 are the same as in E821 as described in [3]. In the present document we describe them and include the main points that aim to improve the muon ring acceptance and reduce muon losses as well as certain systematic errors associated with the coherent betatron oscillation frequencies.

Mechanical Design

Fig. 13.1 shows a schematic top view of the muon $(g-2)$ storage ring indicating the location of four ESQ Q1-Q4 inside the scalloped vacuum chambers. Ideally, the ESQ plates should fill as much of the azimuth as possible, but space is required for the inflector and kicker magnets. For symmetry reasons, the quadrupoles are divided into four distinct regions Q1-Q4. Gaps at 0° and 90° for the inflector and kicker magnets, along with empty gaps at 180° and 270° provide a four-fold symmetry. Overall, the electrodes occupy 43% of the total circumference. The four-fold symmetry keeps the variation in the beta function small, $\sqrt{\beta_{\max}/\beta_{\min}} = 1.04$, which minimizes beam "breathing" and improves the muon orbit stability.

Each quad segment consists of a "short" quad of 13° and a "long" quad of 26°, (see Fig. 13.2), for two reasons: 1) to make every quadrupole chamber independent of others, facilitating their development, testing, etc., and 2) to reduce the extent of low energy electron trapping. Therefore there are two high voltage vacuum-to-air interfaces for each quadrupole segment.

A schematic representation of a cross-section of the electrostatic quadrupoles is shown in Fig. 13.3 with the various dimensions indicated. Shown are the four flat aluminum plates ("electrodes") symmetrically placed around the 90-mm-diameter muon storage region. The four NMR trolley rails are at ground potential. Fig. 13.4 shows a picture of the quadrupoles at the downstream end of one chamber. Fig. 13.5 shows one segment of the muon $(g-2)$ electrostatic quadrupoles at BNL outside its vacuum chamber.

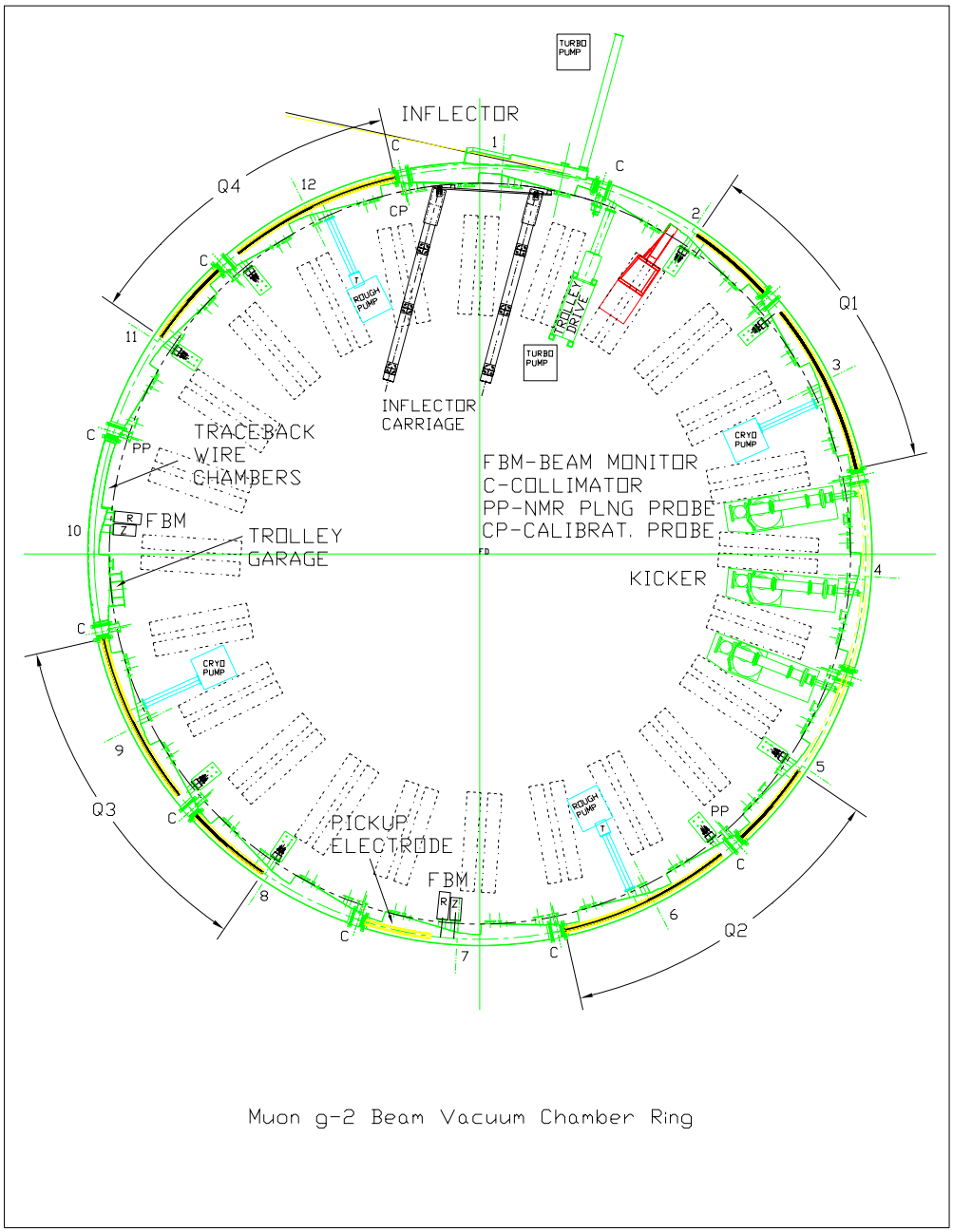

Figure 13.1: A schematic view of the muon $(g-2)$ ring as well as the location of Q1, Q2, Q3, and Q4, the four-fold symmetric electrostatic focusing system.

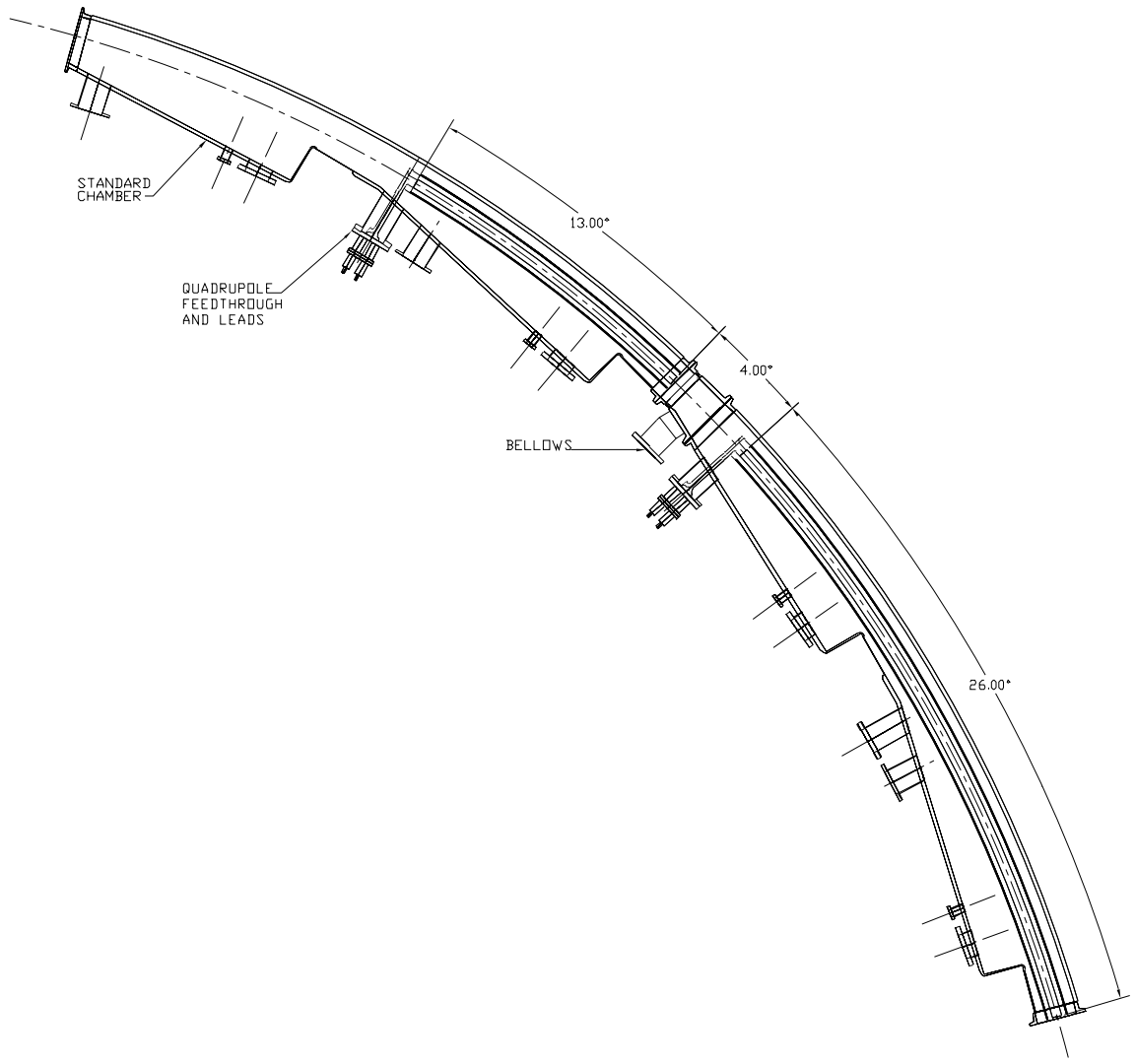

Figure 13.2: A schematic view of a short quad of 13°, and the adjacent long quad of 26°. The high voltage feeding leads break the quad symmetry at the upstream end of the plates to quench the low energy electron trapping and guide them outside the magnetic field region, where they can be released. Some of the bellows are equipped with collimators where the muon beam is scraped immediately after injection.

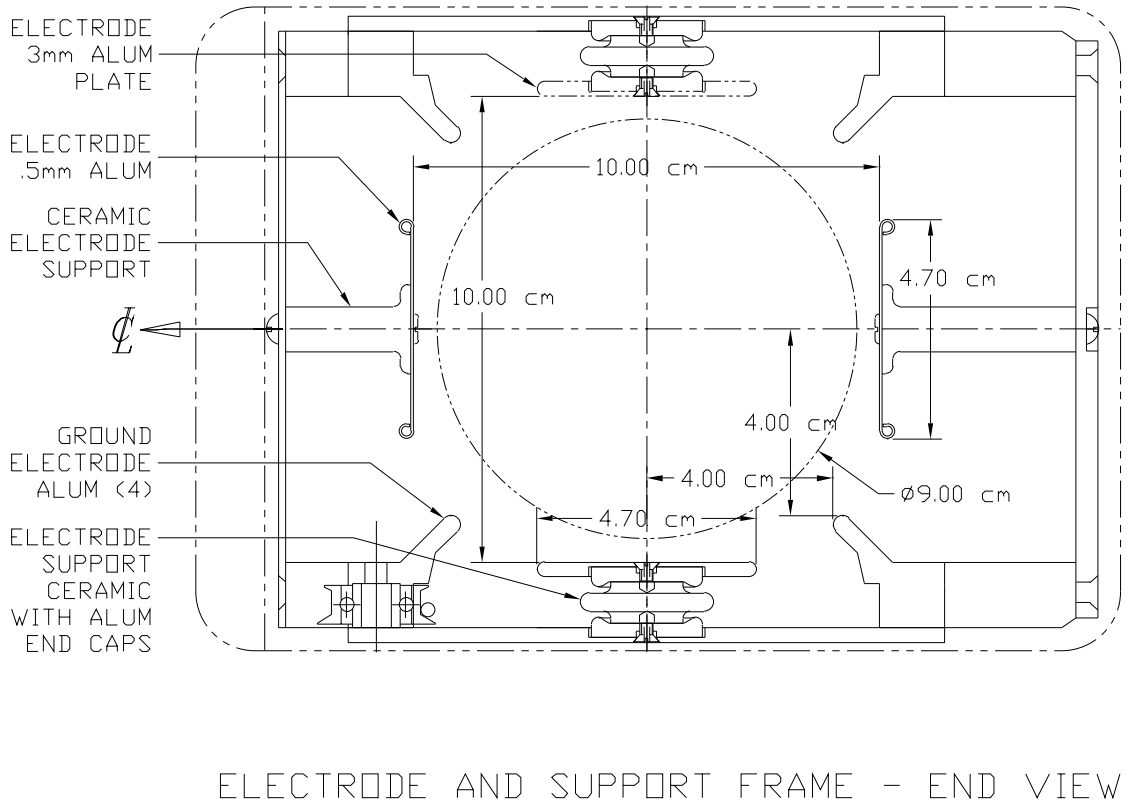

Figure 13.3: A schematic of the quadrupole cross-section. The rails in the corners are kept at ground potential. Most of the side support insulators are replaced with uniform diameter insulators of 0.5 cm.

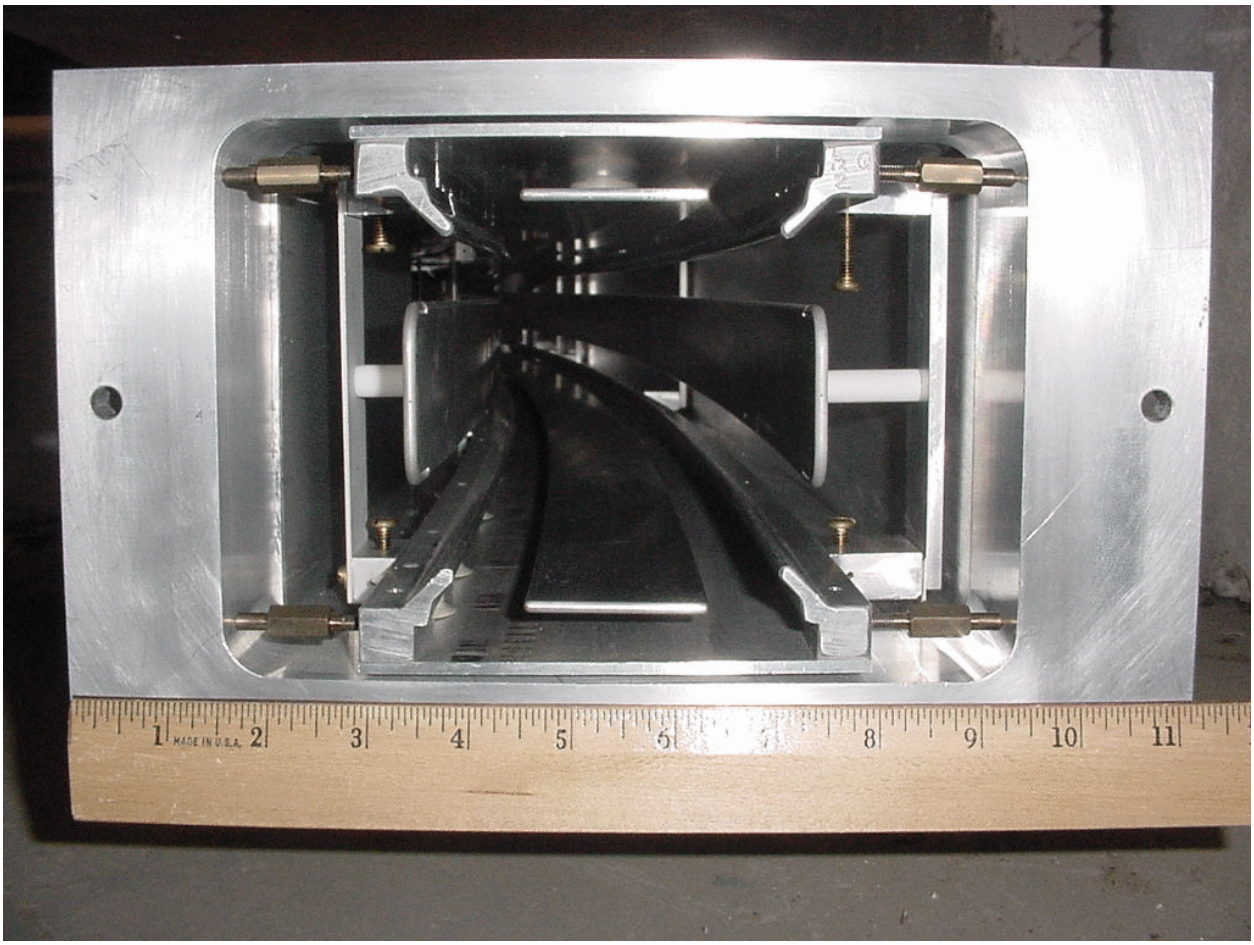

Figure 13.4: A photograph of the downstream end of a vacuum chamber with the cage and quads showing.

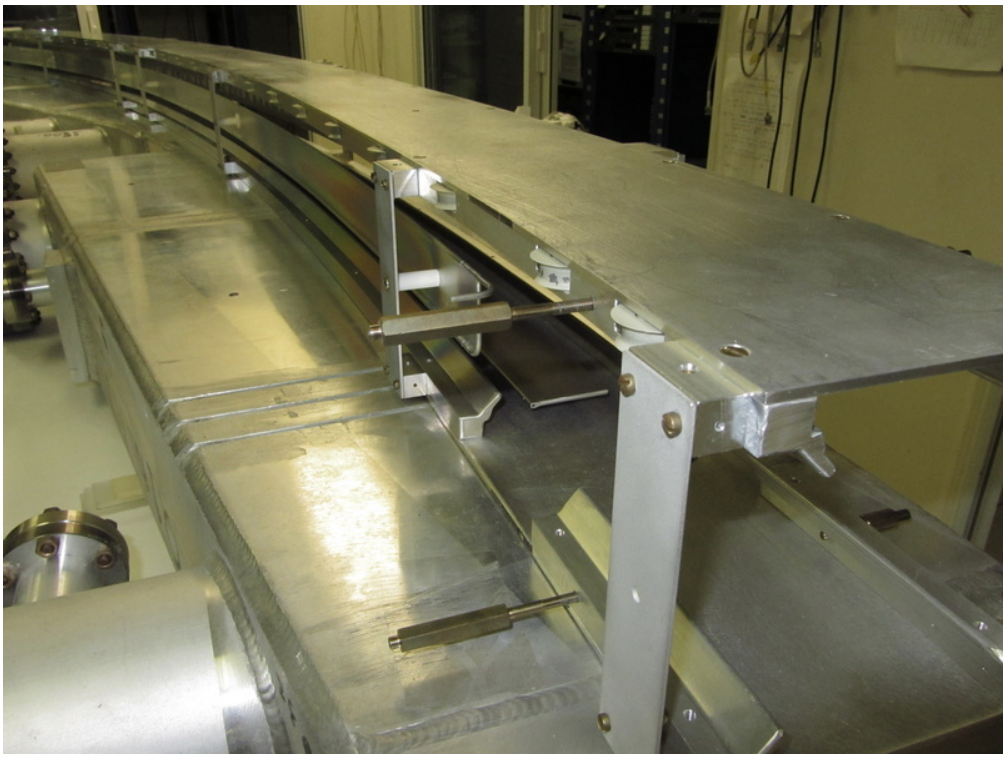

Figure 13.5: One cage (placed here up-side-down) that holds the plates of the electrostatic quadrupoles of the muon $(g-2)$ experiment.

The placement accuracy was 0.5 mm for the horizontal (top/bottom) quad electrodes, and 0.75 mm for the vertical (side) quad electrodes. When measured by the surveyors the electrodes were found to be well within those values.

Electrical Design

The electrical diagram of the quadrupoles is given in Fig. 13.6. The storage capacitance is 1.5 μF, rated at 40 kV [4]. The high voltage (HV) switches are deuterium thyratrons, models CX1585A and CX1591, made by EEV [5], rated at the minimum to 40 kV; and 5 kA maximum current. The baseline plan is to use HV power supplies PS/LKO4OPO75-22 (positive polarity) and PS/LKO4ONO75-22 (negative polarity) from Glassman. They are capable of delivering up to 40 kV at 75 mA maximum [6]. Their voltage regulation is better than 0.005% whereas the ripple is better than 0.025% RMS of rated voltage at full load.

The capacitance of the distribution cables (RG35B) is between 1 and 3 nF depending on how many quadrupole plates are fed, deployed in the star configuration, by the same HV pulser unit. There are four pulser units, two for applying standard high voltage (i.e. a single voltage value per pulse), one for each polarity, and two for scraping high voltage (i.e. two different voltage values per pulse), again one for each polarity. Following the E821 scraping scheme [3], two of the quadrupoles will be used to scrape the injected beam horizontally, by moving the beam sideways, while all the quadrupoles will be used to scrape the beam vertically.

HV monitors will be used to record traces of voltages on the quadrupole plates. Their location is indicated in Fig. 13.6. Fig. 13.7 shows the (home-made) HV monitors output waveforms as recorded by an oscilloscope. Voltage traces from each pair of quadrupole plates will be continuously digitized during each fill at 25 MHz sampling rate using 8-bit 500 MHz waveform digitizers originally built by the Boston University for the MuLan experiment. The sampling frequency of digitizers will be downgraded for E989.

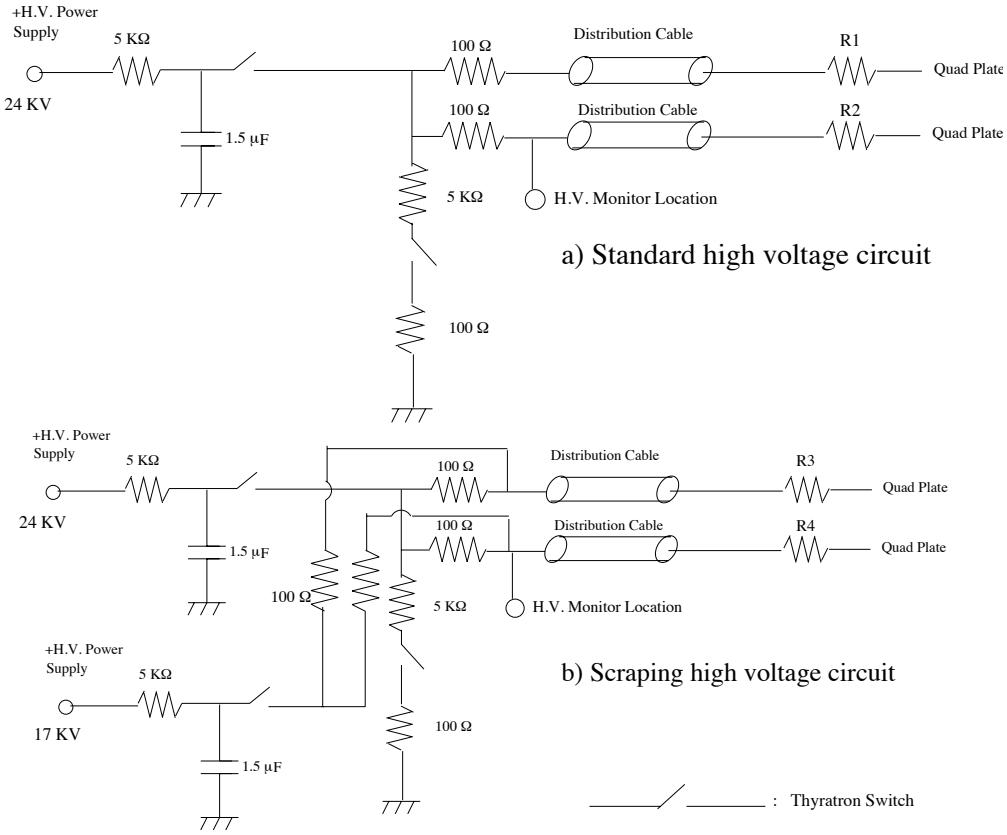

Figure 13.6: A schematic of the scraping and standard HV pulsing systems. The Thyratron switch model used in E821 was the CX1585A produced by English Electric Valve, good to 40 kV.

13.4 Design of Beam Collimators

Beam collimators in the $(g-2)$ storage ring are used to remove muons outside the 9-cm-diameter storage region. In E821 the collimators were 3-mm-thick copper rings having inner and outer radii of 4.5 and 5.5 cm. Eight collimators were installed around the storage ring, the locations are indicated in Fig. 13.8. As will be discussed below, to reduce systematic uncertainties, the design of collimators will be improved in E989, new collimators will be manufactured. In E821, the inner half circles of some collimators were removed to avoid scattering of those low-momentum muons which, because of limitations of the kicker, would otherwise strike the collimator on the first turn and be lost. A photograph of one of the

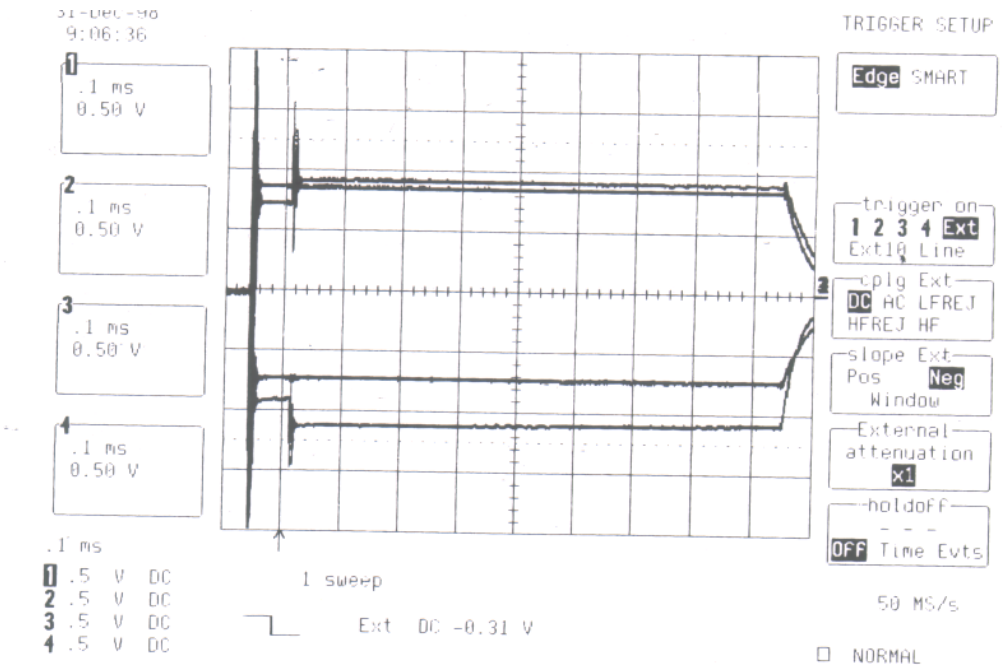

Figure 13.7: The output of the HV monitors as recorded by the oscilloscope.

half-aperture collimators is shown in Fig. 13.9. In E989 the kicker will have enough strength, therefore all half-collimators will be replaced by full-collimators. To improve the efficiency of collimators, the thickness of collimators in E989 will be increased [7]. The optimal thickness will be found as a compromise between conflicting requirements to the collimators, provide efficient scraping of the beam muons and have low distortion of the magnetic field and low scattering of the decay positrons. The studies will be completed by the Final Design.

Muons outside the storage region hit the collimators, lose energy and are lost after several turns. In a storage ring with perfectly uniform dipole magnetic field and ideal quadrupole focusing, no further beam losses occur. In reality, the higher field multipoles provide a perturbative kick which causes some muons to eventually be lost during the measurement period. Muon losses distort the shape of the decay time histogram and can bias the ω_a determination. To reduce such losses the beam is *scraped* to create about 2-mm-wide buffer zone between the beam and collimators. During scraping the quadrupole plates are charged asymmetrically to shift the beam vertically and horizontally and move the edges of the beam into the collimators. After scraping the plate voltages are symmetrized to enable long-term muon storage. We are also studying an alternative scraping method based on excitation of Coherent Betatron Oscillations (CBO). Muons with trajectories close to the beam collimators can be removed from the storage ring by amplifying the amplitude of their betatron oscillations and making them to hit the collimators. The excited CBO will then be damped by applying counter-perturbation. CBO excitation and damping can be accomplished by pulsing a pair of dedicated plates (quadrupole, kicker or custom-built plates) at the CBO frequency.

The collimators can be manually rotated into the "beam position" for data taking, or into the "out-of-beam position" to run the NMR trolley around the storage ring for mapping

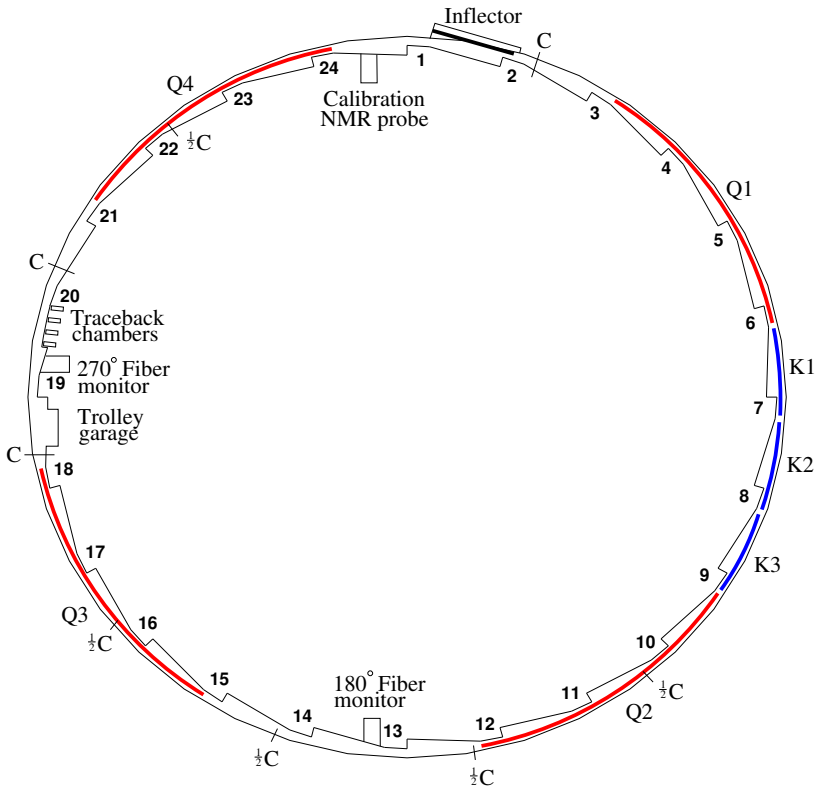

Figure 13.8: Schematic diagram of the E821 ring showing the location of the half and full collimators. For the FNAL experiment, there will only be full collimators.

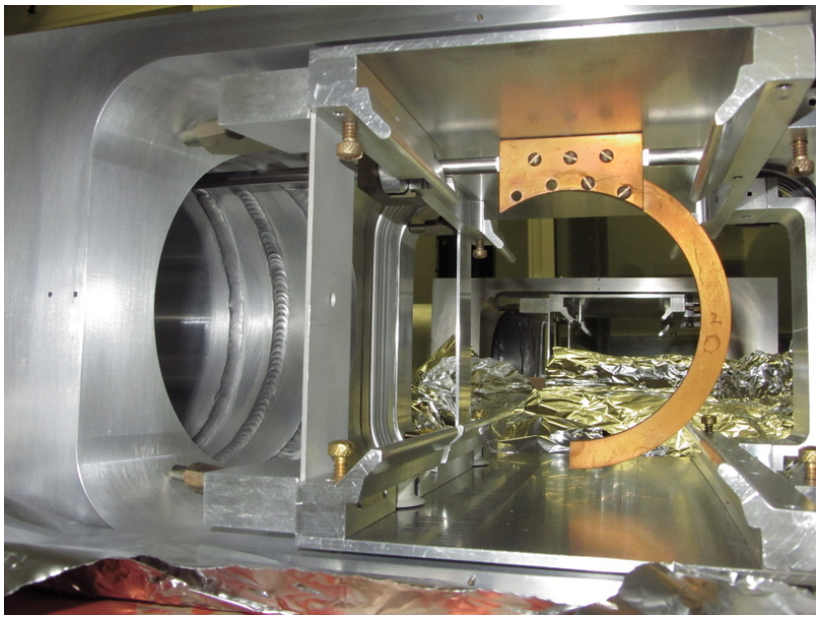

Figure 13.9: Photograph of a half-aperture beam collimator from E821.

the storage magnetic field. For E989 we are planning either to fully automate the rotation of collimators or to install sensors of collimator rotation status. The information on the status of collimators will be important in preventing human mistakes by inhibiting trolley operations if one of the collimators is in a wrong position.

13.5 Beam Polarity and ESQ

The great success of the quadrupole system is based on the fact that it allowed the storage of positive and negative muons for more than 0.75 ms in the storage ring, even though the azimuthal quad coverage was almost half that of the last muon $(g-2)$ experiment at CERN. The vacuum requirements were in the low 10^{-6} Torr for the positive muons and low 10^{-7} Torr for the negative muons. Higher vacuum pressures were tolerated for limited operation periods. Those requirements allowed a speedy recovery after any unavoidable opening up of the vacuum chambers during the initial stages of the runs, related mostly to issues other than the quadrupole operations.

For E989 we focus on positive muon storage only, due to the following advantages:

- It allows us to improve the E-field quality by restoring the normal quadrupole field in the lead region. The plan is now to connect the leads at the center of the plates, expose the E-field from the leads for a couple of centimeters, and, if practical[1], hide them behind a ground shield. The aim is to shield the muon storage region from the E-field generated by the leads.

- Due to the relaxed vacuum requirements associated with μ^+ running, we will be able to raise the high voltage and keep it there for longer times. This may have an impact on the muon lifetime measurement or other systematic error measurements.

- For E821, the quadrupoles required a lengthy conditioning period (a couple of hours, depending on pressure) after every trolley run. For positive muon storage, plus an automated conditioning system, we expect to minimize this recovery time by a factor of two to three. Quadrupole conditioning is much more straight forward in the positive polarity than in the negative polarity. The main reason is that in the negative polarity the support insulators are intercepting the low energy trapped electrons, which, depending on the trapping rate, could cause sparking. The conditioning process in the negative polarity was very delicate and lengthy. One of the possible models for why it worked was that the slow conditioning creates a thin conducting layer on the insulator surface, allowing them to slowly move and thus avoid accumulating a critical level. For the positive polarity there are no insulators in the way of the trapped electrons. We will write a computer software program that will be able to condition the quadrupoles taking into account the vacuum pressures and sparking history.

- For positive muon storage we expect the voltage on the plates to be more stable as a function of time and from pulse to pulse.

[1]Preliminary Design studies indicate that unshielded HV leads have little effect on beam dynamics. Since the space is very tight, we will reevaluate the need and feasibility of shielding during the Final Design.

13.6 ESQ Improvements for E989

Quad upgrade and testing aims to produce an ESQ focusing system that maximizes muon statistics and minimizes potential systematic errors. A large number of improvements will be implemented to ESQ system based on the experience we accumulated during E821 operations. For E989 we require improvements in a number of areas:

1. Operate the quadrupoles at a higher n-value to primarily change the horizontal coherent betatron oscillations (CBO) frequency away from near twice the muon $(g-2)$ frequency. The CBO frequency, being very close to twice the $(g-2)$ frequency, see Table 13.1, pulled the $(g-2)$ phase and was a significant systematic error that required special attention during data analysis. We aim to operate at $n \approx 0.18$ to reduce it by more than a factor of three. Other improvements, e.g., properly matching the beamline to the storage ring (requiring a proper inflector channel) is expected to reduce it by at least another factor of three. Overall the CBO systematic error can be reduced to the level required by E989.

2. Reduce the muon losses by more than an order of magnitude to reduce the Lost Muon systematic error. We will achieve this goal by moving the operating point to $n \approx 0.18$, beam scraping by 2.6 mm in the horizontal and vertical directions after injection, and by keeping the radial B-field below 50 ppm (this level of radial B-field displaces the average vertical position by about 2 mm). The region around $n = 0.18$ is more resonance free than the previous n-values we ran with, see Fig. 13.10. We will refine the quadrupole operating mode by running precision beam dynamics tracking simulations to more accurately predict the muon population phase-space after scraping.

3. Shield the muon storage region from the modified quadrupole field due to the HV feeding lead geometry. This region is less than 5% of the good quad coverage around the ring, but it can still influence the muon loss rate. Preliminary Design studies indicate [8] that the effect on beam dynamics is small, therefore, this is a low priority task.

4. The quadrupole voltage monitors were home-made with limited success in achieving an adequate frequency compensation. We now plan to equip every quad plate (32 in total) with a commercially available frequency compensated HV monitor. This will improve the voltage stability readout by an order of magnitude. In addition, we will cross-calibrate the frequency compensation of each monitor with the electric field in the quad region measured using the Kerr effect.

5. Improve the reliability of the HV-vacuum interface regions with a goal of reducing sparking by at least an order of magnitude. The base design is to cover the interface with dielectric shielding capable of holding high electric fields. Alternative design calls for increasing the spacing between positive and negative leads in the air side of the interface or switching to oil-filled air-vacuum interfaces.

6. The outer Q1 plate and support insulators are estimated to have reduced the stored muon population by about 40%. We now plan to address the muon loss issue by a number of alternative modifications which will be discussed below.

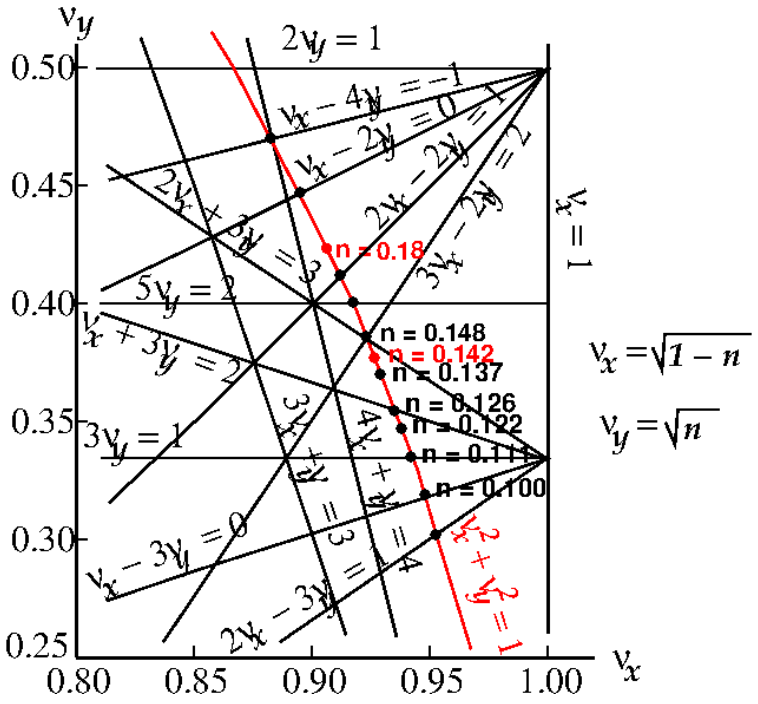

Figure 13.10: The vertical vs. horizontal tune plane together with a number of potential resonance points. The $n-$values $n = 0.142\,; 0.18$ are indicated in red. $n = 0.18$ lies between the resonance lines $\nu_x - 2\nu_y = 0$ and $2\nu_x - 2\nu_y = 1$.

7. Measure the plate vibration during pulsing and stiffen the plate support as needed.

8. Mechanical improvements of ESQ system include

   - increasing the rigidity of quadrupole cages;
   - modification of bolted connections between the parts of quadrupole cages to simplify alignment;
   - improvement of alignment screws (see Figs. 13.4, 13.5);
   - grinding the inner sides of bellow sections to flat to make them more suitable for alignment purposes (see adjustment screws in Fig. 13.9);
   - improving the rigidity of top and bottom quadrupole plates (see Fig. 13.4) against vibrations due to pulsed HV. Preliminary Design studies indicate [9] this is a non-negligible effect, therefore we will continue to investigate this problem and develop a solution. The solution can be as simple as relocating the HV standoffs by 10-20 cm towards the ends of the plates.

All labor-intensive mechanical modifications of the ESQ system, alignment and survey will be performed at Fermilab. Design, R&D studies and prototyping will be pursued at BNL.

Table 13.1: Comparison of high-n and very high-n values.

Parameter	**n=0.142**	**n=0.18**
horizontal tune, ν_x	0.926	0.906
vertical tune, ν_y	0.377	0.425
$f_{\rm CBO}$	495 kHz	634 kHz
$f_{\rm CBO}/f_a$	2.15	2.76
$1/(f_{\rm CBO} - 2f_a)$	27μs	5.7μs
HV	25 kV	32 kV

13.7 Upgrade to Higher n-Value Operation

The maximum voltage we used during the muon runs on the ESQ of E821 was 25.4 kV, resulting in a field focusing index of 0.144. We now plan to raise the maximum voltage to 32 kV for a field focusing index of $n \approx 0.18$. We expect that the higher n-value will

1) increase the ring admittance and most likely the muon storage efficiency;
2) reduce the muon losses during storage;
3) reduce the coherent betatron oscillation (CBO) systematic error.

We will test the quads up to 35 kV, about 10% higher voltage than the anticipated nominal voltage level.

The main issue in E821 was to be able to hold the high voltage without sparking for about 1 ms. This is a very demanding task, especially for storing negative polarity muons, due to low energy electron trapping in the quad region. We were able to achieve this task by designing the HV feeding leads in a way to quench the low energy electron trapping, see Figs. 13.11, 13.12, 13.13.

Vladimir Tishchenko is the L3 manager for the ESQ system and Yannis Semertzidis was the former L3 manager for the same system. The ESQ system currently consists of 8-chambers, 4-pulser systems, 6-HV-power supplies, and a HV monitoring system. To upgrade the ESQ system to higher operating voltage we will:

- Refurbish the HV pulsers to operate at a maximum voltage of $\pm$35 kV, from the present $\pm$25 kV used in E821.
- The side insulators are all varnished due to the negative muon operation at BNL, see Fig. 13.14. The insulators will be either cleaned or will be replaced by new ones.
- Optimize the ESQ for positive polarity muon storage. The leads will be re-configured to quench the low energy electron trapping more efficiently aiming to achieve higher electric field gradient by 30% compared to E821. Achieving this goal will help eliminate the CBO systematic error as well as substantially reduce muon losses.
- Expand the HV vacuum chamber/air interface tube aiming to significantly reduce the sparking in the vacuum side of the leads.
- Modify the geometry of the HV–vacuum interface to reduce sparking in the air side of the HV lead system or immerse it in oil that can withstand the E-field strength.

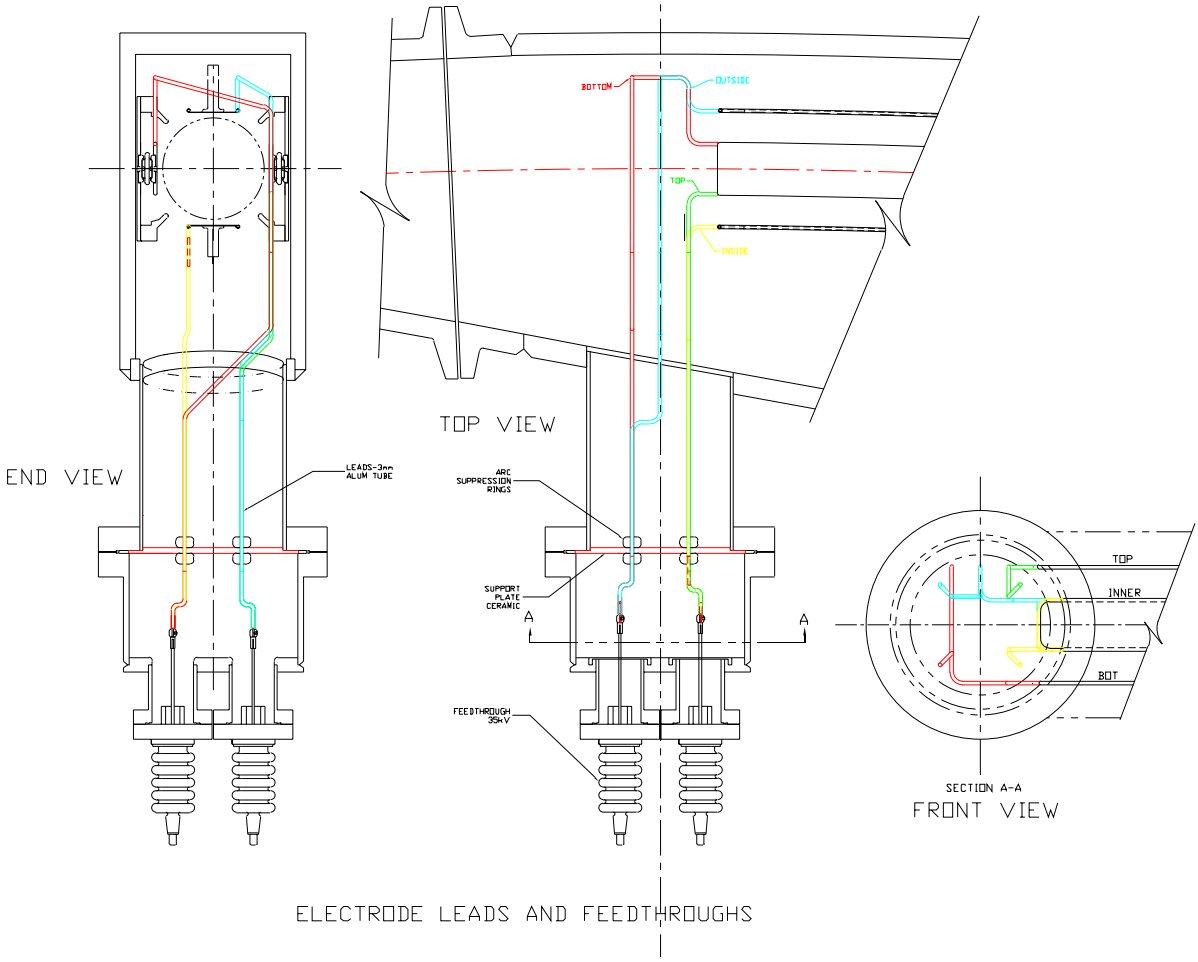

Figure 13.11: Various aspects of the quadrupole high voltage feeding lead geometry, designed to minimize low energy electron trapping.

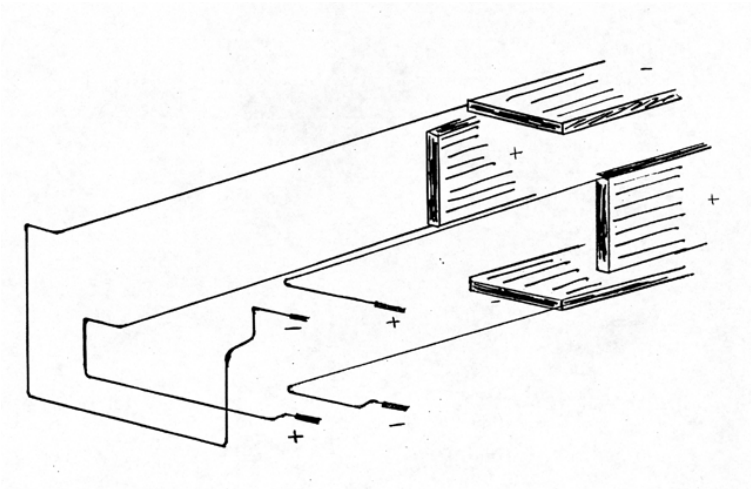

Figure 13.12: Early stages of a hand drawing indicating the high voltage feeding lead geometry.

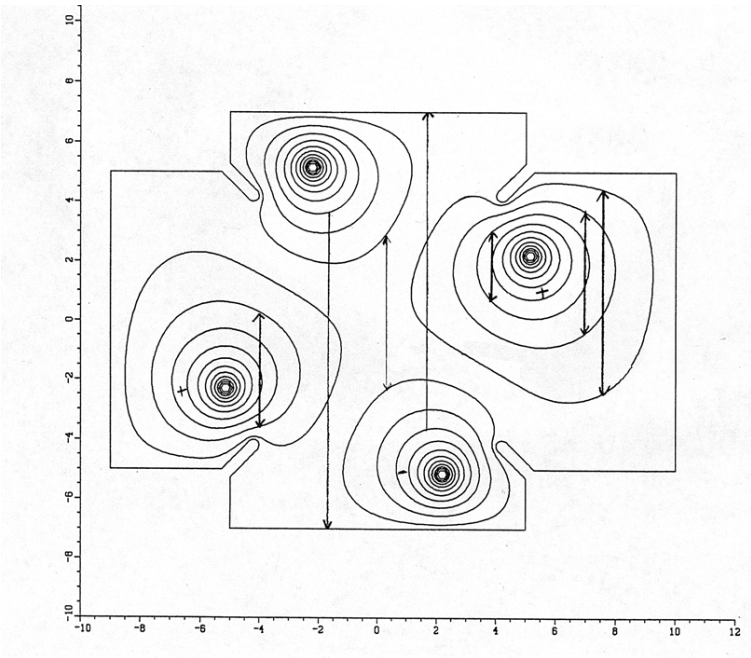

Figure 13.13: A cross section of the lead geometry (vertical [cm] vs. horizontal [cm]). The schematic shows the equipotential lines from an OPERA calculation as well as the low energy electron trapping regions derived from energy conservation. The lead-geometry was designed to optimize the quenching of the electron trapping for the negative muon storage polarity.

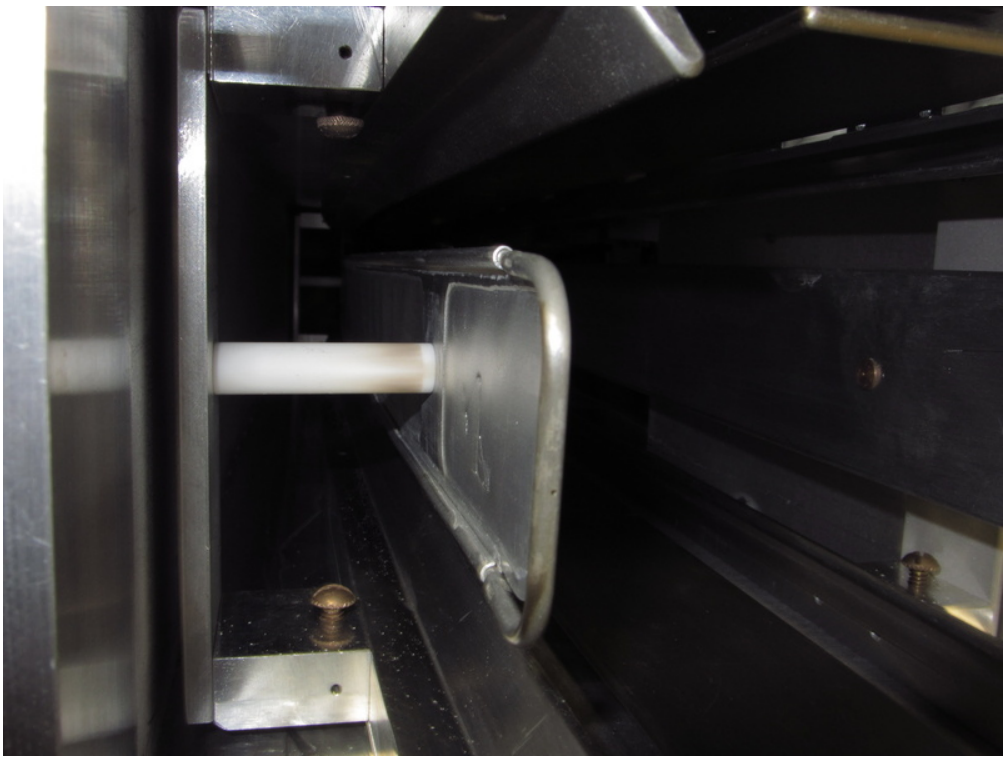

Figure 13.14: The side support insulators are varnished due to trapped electron obstruction during negative muon operations at BNL (darkened appearance close to the plate).

The later is applied routinely in HV applications but it is harder to gain access to it. The sparking rate in the positive polarity in E821 was dominated by sparks at those locations (approximately one spark per 0.5-1 million pulses).

- Shield the electric field generated by the leads from the muon storage region.
- Measure or place strict limits on the magnetic field generated by the trapped electrons.
- Calibrate the pulse shape output of the commercial HV monitors by measuring the electric field generated by the plates using the Kerr effect. The bandwidth (BW) of the Kerr effect measurement is in the GHz range and therefore it is not limited by the level of frequency compensation due to the large capacitance of the components involved.
- Measure the vibration parameters of the quadrupole plates when pulsed using a laser light and a split diode detector. The quad plates can flex under the electromagnetic forces when pulsed. This flexing is (crudely) estimated that it can be of order 10 mm if the pulse duration is of order 1 s. However, for 1 ms the plates can only move by about 10 μm, much below our specs. We will setup a laser system to measure the plate motion due to the impulse of the electrostatic pulse.

During Preliminary Design the beam dynamics studies were performed to ensure that the new higher-n operating point is located far from major betatron and spin resonances [10, 11]. Ref. [10] suggested $n = 0.185$ for E989 as being safely below the $N = 3$ CBO observational resonance at $n = 0.196$. Analysis of betatron resonances around $n = 0.185$ indicated that in the region between $n = 0.17$ and $n = 0.198$ only 6^{th}-order or greater resonances exist which are weak [11]. During adiabatic transitions from scraping to production regimes in E821 the $(g-2)$ storage ring had to cross $\nu_x + 3\nu_y = 2$ resonance (see Fig. 13.10). Resonance crossing lead to partial population of space cleared during scraping. For E989 we will try various scraping voltages in order to find the optimal figure of merit.

In the region $n \approx 0.18$ there is a $k = 0, i = 0, j = -2$ spin resonance at $n = 0.1865$ that would be driven by a radial or longitudinal magnetic field which goes as $x^i y^j \cos(ks/R)$. The analysis showed [11] that field focusing index $n = 0.185$ provides safe operation point.

13.8 Upgrade of ESQ Q1

According to `Geant4` simulations [12, 13], the outer plate of quadrupole Q1 and support insulators reduce the fraction of stored muons by about 40%. The baseline plan of addressing the muon losses is to relocate the outer plate of Q1 from $x = -5$ cm to $x = -7$ cm to allow for the uninhibited injection of the muon beam. Fig. 13.15 shows the `OPERA` model of the quadrupole plates in a quadrupole cage. The plate width is adjusted so that only the normal quadrupole field is dominant, and the 20-pole is kept at the 2% level. Every other multipole is below 0.1%, including the sextupole, octupole, etc. Fig. 13.16 shows the current plan for providing a "massless" outer Q1 plate, by placing it outside the muon path. In order to restore an acceptable field quality, the plate voltage also needs to be raised by about a factor of two, see Fig. 13.17. Another parameter we can use to improve the field quality is to work

with the plate geometry (width, shape, etc.). The requirement of increasing the voltage by a factor of about two we believe we can achieve in the positive muon polarity and we will test it with the test setup at BNL, and with a magnetic field later on at Fermilab.

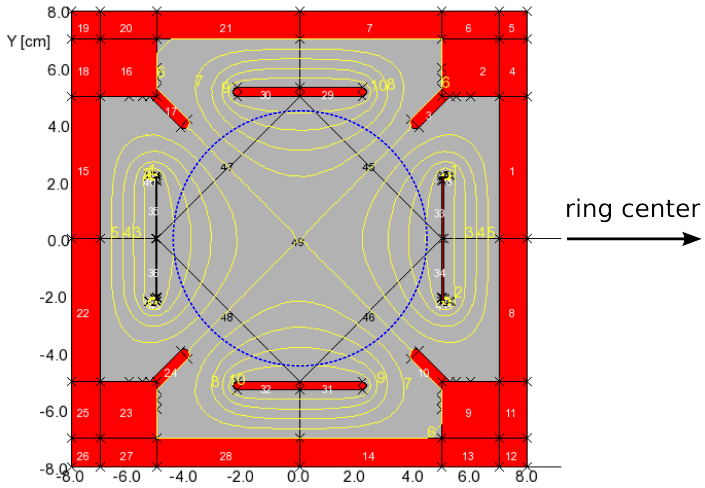

Figure 13.15: An OPERA model of the (normal: Q2, Q3, and Q4) electrostatic quadrupole plates. The top/bottom plates are at a positive voltage and the side electrodes are at (the same) negative voltage. The yellow curves represent the equipotential lines. The 90-mm-diameter muon storage region is indicated by the blue dashed circle.

Since a very high voltage (up to 70 kV) is needed to maintain acceptable quality of the quadrupole field, we are planning to operate the Q1 outer plate at a DC voltage. The horizontal scraping will be accomplished by quadrupoles Q2 and Q3.

13.9 Coherent Betatron Oscillations Systematic Error

The average position and width of the stored beam can vary as a function of time as the beam alternately focuses and defocuses in the ring. This is the result of a mismatched injection from the beam-line into the $(g-2)$ ring via a narrow line, the so-called inflector magnet. This imposes an additional time structure on the decay time spectrum because the acceptance of the detectors and the $(g-2)$ oscillation phase depends on the position and width of the stored muon ensemble.

The CBO frequency in E821 was close to the second harmonic of ω_a, so the difference frequency $\omega_{\rm CBO} - \omega_a$ was quite close to ω_a, causing interference with the data fitting procedure and thereby causing a significant systematic error (see Chapter 4). This was recognized in analyzing the E821 data set from 2000. In the 2001 running period the electrostatic focusing field index, n, was adjusted to minimize this problem. This greatly reduced the CBO systematic uncertainty. We will follow this strategy again but this time we will increase the quad voltage by another 30% to decrease the CBO systematic error by more than a factor of three, see Fig. 13.18.

In addition, the anticipated new kicker pulse shape will better center the beam on orbit. On the detector side, we plan to increase the vertical size of the detectors compared to E821

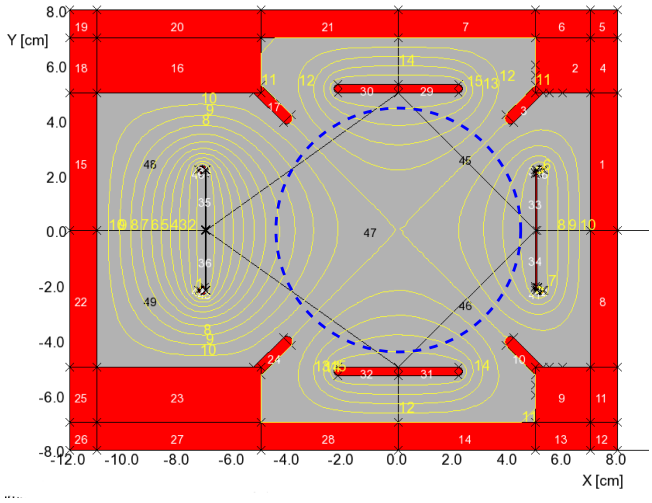

Figure 13.16: An OPERA model of the electrostatic quadrupole plates for Q1. The left plate is displaced to the outside by 2 cm to allow the muons to enter the storage region without having to cross the plates or the support insulators. In order to restore a good field quality (indicated by the symmetric equipotential lines in the center region), the voltage on the left plate is about twice that on the right plate. The 90-mm-diameter muon storage region is indicated by the blue dashed circle.

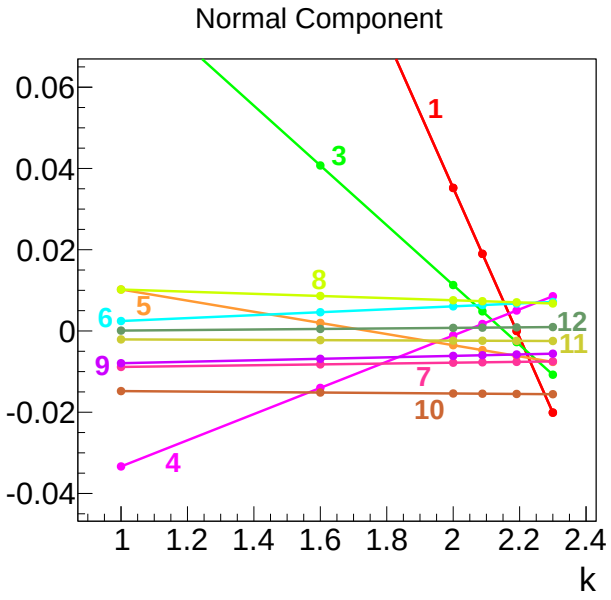

Figure 13.17: Results from OPERA as a function of the voltage multiplication factor for the displaced (outer Q1) plate. Most of the multipoles are below 1% but not all.

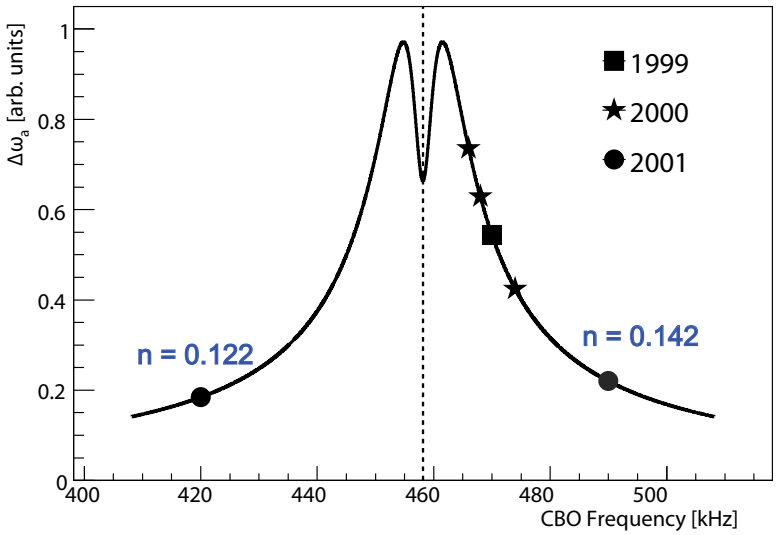

Figure 13.18: The CBO systematic raw error (arbitrary units) as a function of CBO frequency. The year notation indicates the frequencies ran with in E821. For E989 we plan to use much higher field focusing index (see quad section) with a projected CBO frequency of 634 kHz. This frequency will significantly reduce the CBO systematic error.

(from 14 to 15 cm). This reduces the fraction of lost electrons passing above or below the detector, and therefore the sensitivity of the detector acceptance to beam position and width.

In an ideal world, where the detector resolution is uniform around the ring, the CBO systematic error averages to zero when all the detected positron pulses are summed up. However, for E821 the kicker plate geometry broke significantly the detector resolution symmetry around the ring resulting to a non-zero average. With the new design we expect to significantly restore this symmetry.

The combined efforts should reduce the CBO uncertainty by at least a factor of four to well below 0.02 ppm. If a new inflector with wider horizontal aperture is used, then it is feasible to eliminate the CBO systematic error to well below our sensitivity level.

13.10 Collimators and Lost Muon Systematic Error

The E821 lost muon systematic error was 0.09 ppm. In this section we discuss how we will decrease the lost muon rate with an improved storage ring/collimator system. The distortions of the vertical (y) and horizontal (x) closed orbits (CO) due to radial (B_r) and vertical B_y multipole magnetic field distortions are:

$$\Delta y_{\rm CO} = \sum_{N=0}^{\infty} \frac{R_0}{B_0} \frac{B_{rN}\cos(N\Theta + \phi_{yN})}{N^2 - \nu_y^2} \tag{13.1}$$

$$\Delta x_{\rm CO} = \sum_{N=0}^{\infty} \frac{R_0}{B_0} \frac{B_{yN}\cos(N\Theta + \phi_{xN})}{N^2 - \nu_x^2}\,, \tag{13.2}$$

Table 13.2: Distortion of the closed orbits for E821 (FNAL) tune values and B_{rN}/B_0 and $B_{yN}/B_0 = 10$ ppm.

N	y_{CO} (mm)	x_{CO} (mm)
0	0.53 (0.40)	0.08 (0.09)
1	0.08 (0.09)	0.53 (0.40)
2	0.02 (0.02)	0.02 (0.02)
3	0.01 (0.01)	0.01 (0.01)

where N is multipole component, $R_0 = 7112$ mm is equilibrium radius, $B_0 = 1.45$ T is central value of the dipole magnetic field, ν_x and ν_y are horizontal and vertical tunes, respectively.

For E821, the average radial magnetic field B_{r0} drifted by typically 40 ppm per month, which was correlated with temperature changes. About once a month B_{r0} was adjusted with the current shims to maximize the number of stored muons, i.e., centering the beam vertically in the collimators. From equ. (13.1) $B_{r0}/B_0 = 40$ ppm changes the vertical closed orbit by 2 mm. At FNAL we plan much better temperature control compared to E821. B_{y1}/B_0 was shimmed to < 20 ppm, which distorted the horizontal closed orbit by < 1 mm. For the FNAL experiment, we want both of these components < 10 ppm. Other components are less important since $\nu_y^2 \approx 0.18$ and $\nu_x^2 \approx 0.82$ are closest to the integers 0 and 1, respectively (see Table 13.2). For E821 we used $\nu_y^2 \approx 0.13$ and $\nu_x^2 \approx 0.87$.

The E821 collimators were circular with radius 45 mm. The E821 beta functions vs. ring azimuth are shown in Fig. 13.19. The FNAL experiment collimators will be oval with the x and y axes modulated by the square root of the beta functions, i.e., ± 0.8 mm in x and ± 0.7 mm in y.

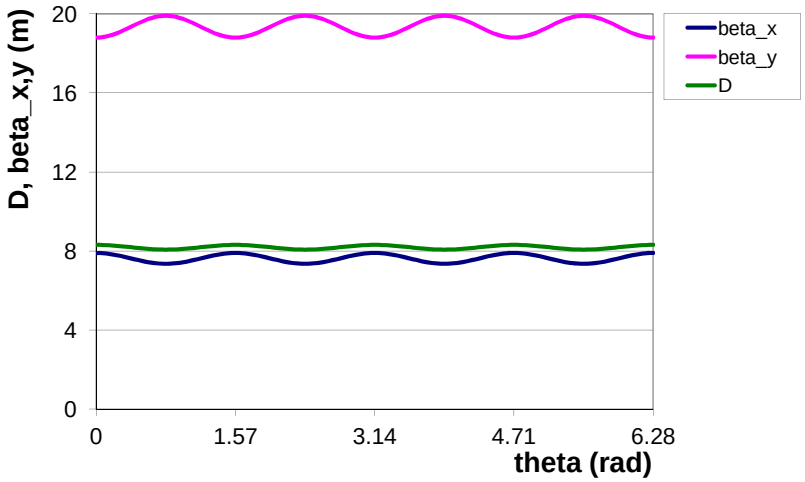

Figure 13.19: E821 horizontal and vertical beta functions.

Fig. 13.8 shows the E821 collimator ring placement. Since the E821 kick extended over many turns, we needed "half" collimators just after the kicker and at π radial betatron

phase advance, so that the muons would survive enough turns to get the full kick. The FNAL kicker is being designed to give the full kick on the first turn. Thus we can go from 3 full collimators and 5 half-collimators to eight full collimators.

We purposely distorted the vertical and horizontal closed orbits by 2.6 mm during scraping for the first 10^2 turns, but 2.6 mm was not large compared to the above effects. Indeed, when there were large temperature variations, we sometimes observed that the lost muon rate went *up* after scraping ended(!), which can happen in the presence of a significant radial B-field with proper polarity. With better control over the horizontal and vertical orbit distortions due to B_{r0} and B_{y1}, oval collimators to match the ring beta functions, and eight full collimators, we anticipate a lost muon rate at FNAL which will be about ten times lower than E821. The exact lost muon rates will be calculated with tracking simulation. The collimator positions should be surveyed to better than 0.3 mm. The coefficient of expansion of steel is 1.3×10^{-5}/C; multiplying times the radius of 7.1 m gives 0.1 mm/C.

The collimators are able to be put into the "beam position", or into the "trolley position". The latter is required to run the NMR trolley. We will put one collimator into the beam position and record the lost muon rate with the lost muon detector. This takes about ten minutes of data collection. Then we put a second collimator into the beam position. We will have from simulation how much the lost muon rate should decrease with two collimators perfectly aligned with respect to the closed orbit. If we don't observe this decrease, we will remotely position the second collimator in x and y until we achieve the desired result. Then we put in the third collimator, etc.

13.11 Alignment and Survey

As it was discussed in the previous section, the collimator positions should be surveyed to better than 0.3 mm. The placement accuracy requirements of ESQ plates in E821 was 0.5 mm for the horizontal (top/bottom) quad electrodes, and 0.75 mm for the vertical (side) quad electrodes. When measured by the surveyors the electrodes were found to be well within those values. To improve the quality of quadrupole focusing field and reduce systematic uncertainties we require that the ESQ plates must be positioned and surveyed to 0.3 mm or better. Based on our experience in E821 we believe that this accuracy level is within the reach of modern survey technologies. Mechanical modifications of quadrupole cages summarized in section 13.6 is an important part of improvements that lead to better alignment accuracy.

13.12 Quality of Quadrupole Focusing Field

Due to discrete structure of ESQ, flat geometry of ESQ plates, scalloped vacuum chambers, imperfect placement of ESQ plates discussed in the previous section, etc., the real focusing field of ESQ contains non-quadrupole multipoles. Important considerations of the multipoles of the focusing field include

1. Distortions of the closed orbit which affect

    - ω_p systematic error;

- Lost Muon systematic error;
- Pitch correction systematic error;
- E-field correction systematic error;

2. Betatron resonance excitation which affects the Lost Muon systematic error.

3. Coherent betatron oscillation (CBO) de-coherence, which affects the CBO systematic error.

In order to have acceptable beam dynamics systematic errors, non-quadrupole field multipoles must be kept below appropriate levels. Preliminary specs on ESQ multipoles have been defined by the Preliminary Design studies [14, 15]. Below we give a brief summary of the results.

- **CBO** ESQ field multipoles (presumably the 20-pole) lead to faster CBO de-coherence, which reduces the CBO systematic uncertainty. Potentially one can use this fact to optimize the ESQ field to reduce the CBO systematic error in E989, but more rigorous studies to better understand the effect are under way (see section 4.5.2).

- **Betatron resonance excitation** The closest 20-pole resonance is relatively narrow ($\delta n = \pm 10^{-3}$) and far ($\Delta n \approx 0.02$) from the $n = 0.185$ operating point in E989. Based on systematics measurements in E821, we concluded that this should not be an issue for E989.

- **E-field correction** A preliminary systematics study shows a significant (up to $\Delta\omega_a \approx$ 30 ppb) effect only for non-magic muons (with $\Delta p/p_{\text{magic}} \approx 0.25\%$) with large betatron oscillations ($A_x = 40$ mm). To estimate the effect in the entire E989 data set a realistic data sample of stored muons will be simulated (see section 4.5.2).

- **Pitch correction** The effect is sizable ($\Delta\omega_a \approx 9$ ppb) only for muons with large betatron oscillations $A_y \sim 40$ mm. Like in the previous case, a better estimate will be made when a sample of stored muons will become available.

- $\omega_{\mathbf{p}}$ The expected distortion of the closed orbit due to quad misalignment is $\Delta x <$ 0.2 mm. The "Muon Distribution" component of the total ω_p systematic error will be addressed by improving the uniformity of the storage magnetic field (see section 15.3 for more details).

Summarizing, Preliminary Design studies show that the chosen baseline design of this WBS element meets the systematics goals of the experiment. We will continue our studies during the Final Design to finalize the specs on ESQ plate placement accuracy and magnitudes of field multipoles.

13.13 ES&H

Potential hazards of the ESQ system are power system and X-rays.

The system contains both low voltage, high voltage (up to 75 kV) and high current circuits. There are no exposed electrical terminals. All electrical connections are bolted and enclosed. Cables will either run along the floor in a cable tray or in a double-grounded conduit. The power supplies and the thyratrons are fused. We will use lock out/tag out when servicing the unit. When the power supplies are disabled, the storage capacitors will also be shorted to ground with a safety relay. We do not anticipate that we will need to work on the unit hot. There are no requirements for emergency power. There will be a remote control unit in the control room. The operation of ESQ will be limited to system experts and trained personnel.

Soft X-rays can be produced in the system in spark discharges. Even though the ESQ system is designed to have no sparks during normal running conditions, sparks are most likely to occur during conditioning of the system. Aluminum vacuum chambers with 1-cm-thick walls provided adequate shielding against X-rays in E821. Due to higher operating voltage in E989 the shielding by vacuum chambers may not be sufficient. We are planning to develop an integrated X-ray safety plan together with the kicker group.

One of the alternative designs of the outer plate of Q1 quadrupole includes beryllium foil. Beryllium is ideal material for such purpose due to its mechanical, electrical and magnetic characteristics. Most importantly, muon scattering in beryllium will be significantly reduced in comparison with aluminum plate due to lower Z of beryllium. However, beryllium is a well-known health hazard. We are not planning to machine beryllium in the Lab. The foil will be produced and, presumably, assembled by a certified commercial company. During running the beryllium plate will be enclosed in vacuum chamber inaccessible to regular personnel. Only certified personnel will be allowed to perform work on a modified ESQ Q1.

The ESQ design will be reviewed by the (PPD or AD) electrical safety committee. Proper Operational Readiness Clearance will be obtained before unattended operation of the systems. Job Hazard Analyses will be performed for any work tasks that involve working on the high voltage systems.

13.14 Risks

The baseline design is to displace the Q1 outer plate by about 2 cm (the needed displacement will be determined more accurately by R&D studies). If the baseline design cannot be achieved for various reasons, we will consider the following alternatives for Q1 outer plate, *i)* a plate made from a thin beryllium foil, *ii)* a plate made from a thin wire mesh, *iii)* a plate made from a thinner aluminum foil, *iv)* a plate from other alternative materials (e.g. fiber carbon). This will lead to the following consequences to the Project

- More effort will be needed for R&D studies of alternatives.
- Muon scattering in any material will reduce the fraction of stored muons and hence increase the time required to reach the statistical goal of the experiment. The preferable material is beryllium.
- Beryllium foil will increase the cost of the Project. The cost of the beryllium material for the plate is about \$16 k per meter. Thus, to cover a 5-m-long quadrupole plate at

least \$90 k in addition will be required not including the manufacturing and assembling expenses.

- Beryllium is a hazardous material. Special handling requirements will complicate ESQ plate installation and adjustment procedure.

The baseline design is to increase the operating voltage of ESQ to ±35 kV. The CBO systematic error will be more challenging to address if this goal is not reached. This will also increase muon losses.

The ESQ system requires good vacuum to operate properly (10^{-6} Torr or better). Bad vacuum conditions may lead to inability of ESQ to operate at nominal voltage. One potential source of vacuum leak is the tracker system. If the leak is too large, additional vacuum pumps may be needed to pump the vacuum chambers equipped by the tracker system. If high vacuum conditions are not met with installation of additional vacuum pumps, we may consider taking production data without tracker system and taking special runs with the tracker system to measure the distribution of muons in the storage ring. The disadvantage of such a mode of operation is that the tracker runs will be excluded from the production dataset.

13.15 Quality Assurance

Reliable operation of the quadrupole system is necessary to achieve the experiment's goals. We have planned a testing program that includes computer simulations and extensive hardware testing of the ESQ system in advance to installation into the experiment to insure reliability, and this is accounted for in the cost and schedule estimation.

BNL has established a test stand to assess performance of the ESQ system. The test stand will include vacuum system, high voltage electrical system, high voltage monitors, electrooptic high-voltage system and the data acquisition system. It has already been or will be used to

1. Study the stability of the high voltage with and without magnetic field by pulsing the plates 10% above nominal voltage.
2. Study the mechanical stability of the quadrupole plates under high voltage stress.
3. Perform R&D studies of the Q1 outer plate.
4. Perform R&D studies of high voltage leads.
5. Test the procedure of conditioning the ESQ system.
6. Measure the X-rays exposure level due to sparking.
7. Develop and test the data acquisition system.

We are planning to install the ESQ system a year in advance of the start of the experiment. This will allow us to test the system in real experimental environment and will

give us sufficient time to make alternation if necessary without delaying the schedule of the experiment.

To assure the quality of the future experimental data and to identify potential problems we will continue doing precision computer simulations of two types, `OPERA` simulations of the electric field produced by both quadrupole plates and high voltage leads, and tracking simulations of muons in the electric and magnetic field using `Geant4` and/or independent dedicated tracking program developed by Y. Semertzidis for E821. The computer simulations are backed up by analytic calculations where possible.

13.16 Value Management

The reference design is lower cost than other alternatives we have considered (see discussion above) and this is the design we will use, provided it meets the requirements. The design process has benefitted from the experience gained in E821.

The baseline design is to re-use the existing E821 electrostatic focusing quadrupoles. Some components require cleaning and refurbishing. To meet the statistics goal of the E989 experiment and maximize the number of stored muons we are planning to upgrade the outer plate of the quadrupole Q1. To meet the systematics goals of E989 we are planning to modify some components of the ESQ system (improve rigidity of ESQ cages to meet new requirements on alignment precision, redesign high voltage leads to provide the electrostatic field of better quality, upgrade some components of the high voltage power system to enable operation at higher field focusing index, etc.). Where possible, the upgrade will reuse the existing components from E821.

We are planning to re-use the existing Boston waveform digitizer electronics used in muon lifetime measurements by the MuLan collaboration [16]. The digitizers will be used to record HV traces from each quadruple plate (32 channels total).

13.17 R&D

Work is well underway on R&D studies of quadrupole Q1. The `Geant4` simulations conducted independently by N.S. Froemming [12] and T. Gadfort [13] were important in guiding the choice of material for the outer plate of Q1. The preliminary `OPERA` simulations were important in making the choice of the baseline design of quadrupole Q1 (Fig. 13.16). The tracking simulations were important in understanding the muon beam dynamics in $(g-2)$ storage ring with skew and upright quadrupoles [17, 18]. More precision computer simulations will be conducted to finalize required tolerances and to quantify systematic uncertainties related to ESQ system. Extensive tests of a prototype of quadrupole Q1 will be conducted in a test stand at BNL.

References

[1] J. Bailey, *et al.*, Nucl. Phys. B150:1 (1979)

[2] G.W. Bennett, *et al.*, Phys. Rev. D 73, 072003 (2006)

[3] Y.K. Semertzidis *et al.*, Nucl. Instr. Meth. Phys. Res., A 503 (2003) 458-484

[4] High voltage storage capacitors, model RC1207 from RFI Corp., 100 Pine Aire Drive, Bay Shore, L.I., N.Y. 11706.

[5] English Electric Valve, Waterhouse Lane, Chelmsford, Essex CM1 2QU, England.

[6] Glassman High Voltage, Inc., 124 West Main Street, P.O. Box 317, High Bridge, NJ 08829, `http://www.glassmanhv.com`.

[7] W.M. Morse, "E989 Collimator Design", E989 note #1466, `http://gm2-docdb.fnal.gov:8080/cgi-bin/ShowDocument?docid=1466`

[8] W.M. Morse, "Effect of Electric Quad Leads on Muon Beam Dynamics", E989 note #1605, `http://gm2-docdb.fnal.gov:8080/cgi-bin/ShowDocument?docid=1605`

[9] W.M. Morse, "Electric Quad Natural Frequencies", E989 note #1606, `http://gm2-docdb.fnal.gov:8080/cgi-bin/ShowDocument?docid=1606`

[10] I.M. D'Silva and Y.K. Semertzidis, "A Systematic Error Study: The Effect of Coherent Betatron Oscillations on the g-2 Frequency", E989 note #1282, `http://gm2-docdb.fnal.gov:8080/cgi-bin/ShowDocument?docid=1282`

[11] W.M. Morse, "Electric Quad Resonances", E989 note #1888, `http://gm2-docdb.fnal.gov:8080/cgi-bin/ShowDocument?docid=1888`

[12] N.S. Froemming, "Scattering Through Q1 outer", E989 note #567, `http://gm2-docdb.fnal.gov:8080/cgi-bin/ShowDocument?docid=567`

[13] T. Gadfort, "Muon Storage Rate Study", E989 note #920, `http://gm2-docdb.fnal.gov:8080/cgi-bin/ShowDocument?docid=920`

[14] W.M. Morse, "Specs on E989 Electric Quad Multipoles", E989 note #1604, `http://gm2-docdb.fnal.gov:8080/cgi-bin/ShowDocument?docid=1604`

[15] V. Tishchenko, "Electrostatic Focusing Quadrupoles and Collimators: Preliminary Design", E989 note #1750, http://gm2-docdb.fnal.gov:8080/cgi-bin/ShowDocument?docid=1750

[16] V. Tishchenko *et al.* [MuLan Collaboration], Phys. Rev. D 87, 052003 (2013) arXiv:1211.0960 [hep-ex].

[17] Y.K. Semertzidis, "Quadrupoles: Focusing on positive muons", E989 note #914, http://gm2-docdb.fnal.gov:8080/cgi-bin/ShowDocument?docid=914

[18] V. Tishchenko *et. al.*, "Electrostatic Focusing Quadrupoles: Recent studies", E989 note #911, http://gm2-docdb.fnal.gov:8080/cgi-bin/ShowDocument?docid=911